



Bioinspired Hard–Soft Interface Management for Superior Performance in Carbon Fibre Composites

Ben Newman¹ · James D. Randall¹ · Russell J. Varley¹ · Filip Stojcevski² · Luke C. Henderson¹

Received: 10 April 2023 / Revised: 10 April 2023 / Accepted: 24 April 2023 / Published online: 24 July 2023
© The Author(s) 2023

Abstract

Nature has evolved to create materials of unmatched performance governed by the interfacial interactions between hard and soft surfaces. Typically, in a carbon fibre composite, one polymer and one type of carbon fibre is used throughout a laminate. In this work, we use a carbon fibre surface modification approach to vary the fibre–matrix interface throughout the laminate to tailor the soft–hard interfaces. We demonstrate this effect using reclaimed carbon fibre materials in a thermoset polymer, then extend this concept to a thermoplastic polymer matrix–polypropylene. The thermoset specimens examined in this work consist of 5 carbon fibre plies, featuring 0, 1, 3 or 5 surface-modified layers located at the centre of the composite. The largest improvements in physical properties for these composites (yield strength, ultimate flexural strength, and tensile modulus) were found when only 1 modified layer of carbon fibre was placed directly within the centre of the composite. Subsequent investigations revealed that for a polypropylene matrix, where the surface chemistry is tailored specifically for polypropylene, improvements are also observed when mixed surface chemistries are used. This work shows that surface modification of reclaimed carbon fibres as non-woven mats can provide significant improvements in mechanical properties performance for structural composites when used in strategically advantageous locations throughout the composite.

Keywords Carbon fibre · Hybrid interface · Mechanical properties · Recycled composites · Polypropylene

1 Introduction

Carbon fibre-reinforced polymer composites (CFRPs) have become a key material within advanced manufacturing sectors including aerospace, automotive, and renewable energy (wind, hydrogen, etc.) [1–3]. This is largely attributed to their superior properties including high strength, light weight, and corrosion resistance [4–6]. For all their benefits, an inherent weakness with CFRPs remains their susceptibility to delamination and debonding at the fibre–matrix interface [7, 8]. This failure mechanism can be caused by poor chemical compatibility between the inert carbonaceous surface of carbon fibres and the surrounding polymer matrix. Fibre delamination of composite materials [9–11] arises when the stress transfer from the polymer to the fibre

exceeds the adhesive strength between the fibre and polymer. This immediately results in defects, stress concentrations, and voids which further deteriorate material performance resulting in premature failure. It has been proposed that CFRPs have only reached 10% of their theoretical mechanical potential, primarily due to the inability to effectively transfer stress across the fibre-to-matrix interface [12, 13].

The manipulation of the interface and/or interphase within composite materials, however, is an emerging strategy that has been shown to address some of these shortcomings in regard to premature delamination. This is epitomised in the extraordinary properties of natural materials, such as nacre [14, 15], silk [16, 17], and bone [15, 18], among others [19], where the management of the interface between hard and soft materials is critical for the efficient transfer of stress [5, 12]. The optimisation of this hard-soft interface is therefore a strategy which for the development of superior composite materials that are tougher, stronger, and stiffer. The different approaches taken to manipulate the carbon fibre surface include both chemical and physical, including ‘wet’ chemical reactions, electrochemistry, grafting polymers or small molecules, deposition of nanomaterials, and

✉ Luke C. Henderson
luke.henderson@deakin.edu.au

¹ Institute of Frontier Materials, Deakin University, Waurn Ponds Campus, Victoria, Australia

² Department of Industrial and Materials Science, Chalmers University of Technology, Gothenburg, Sweden

plasma treatments, among others [7]. In current carbon fibre manufacturing processes, improving compatibility to the polymer phase is carried out via electrochemical oxidation, which introduces polar oxygenated functional groups to the fibre surface [20–25], and the application of a fibre sizing. The latter is a proprietary cocktail of many constituents (e.g. polymers, anti-static agents, emulsifiers, etc.) that is deposited on the fibre surface [26–28]. This sizing application is typically a thin polymer layer that functions as an intermediate layer between the fibre and the matrix [28–30] and plays a central role in minimising fuzz, improving handling and weaving. When fully optimised, these traditional surface treatments have been reported to improve the interfacial shear strength (IFSS) in epoxy thermosets by 53.8% [31, 32] and up to 14.1% for thermoplastics [33].

In this work, we tailor the surface chemistry of reclaimed carbon fibres to enhance the interfacial adhesion towards both thermoset (epoxy) and thermoplastic (polypropylene, PP) polymer matrices. An amine group has been chosen to complement the thermoset polymer (Fig. 1B), as this is able to undergo cross-linking reactions with the epoxy and has shown to be a reliable surface modification [34–36]. Polypropylene, however, is particularly challenging to reinforce due to its extremely hydrophobic nature and lack of chemical functionality. Nevertheless, it remains a polymer of great interest to use in CFRPs as it is easy to process, chemically resistant, and is produced on vast scales. A recent investigation into electrochemically modified carbon fibres for injection moulded polypropylene parts has shown improvements

of up to 32% in fracture toughness [37]. In this work, we have chosen to tailor the surface chemistry of the fibres to PP by installing an aromatic ring bearing a short alkyl chain (Fig. 1B, 4 carbons, butyl) to complement the aliphatic nature of PP.

2 Experimental

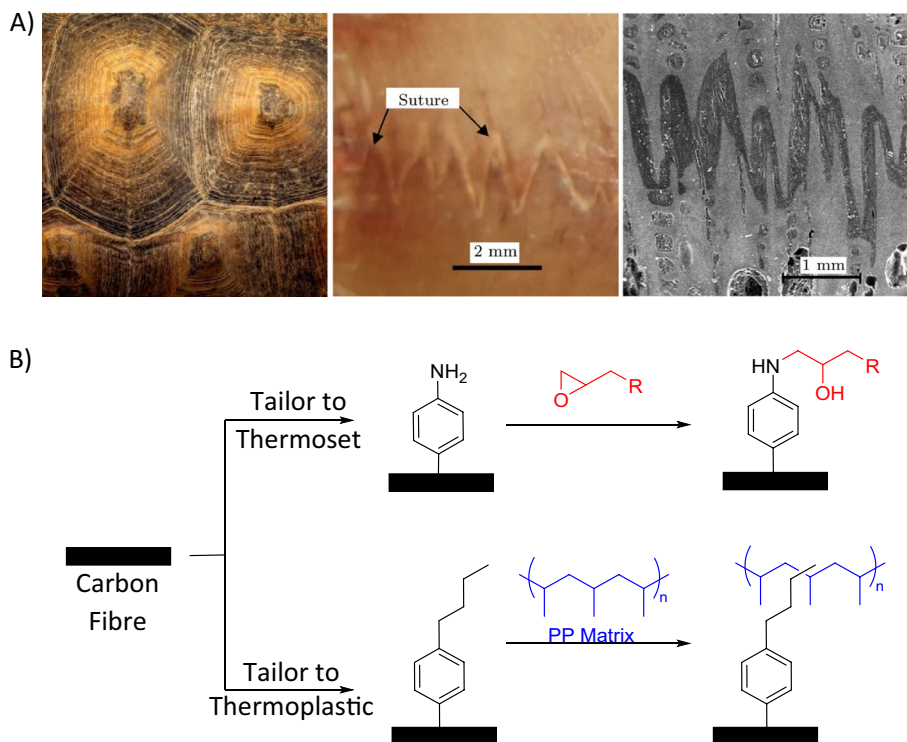
2.1 Materials and Manufacturing

The epoxy resin used was Hexion Epikote (RIM935/RIMH936) prepared as per the manufacturer's specifications. The resin was stored in a cool dry place but were used as received.

2.1.1 Thermosetting Sample Preparation

Modification of a non-woven reclaimed carbon fibre mat for the epoxy resin was carried out as per our previously reported processes. Briefly, the sample to be modified is set as the working electrode in a 3-electrode cell, with a carbon fibre counter electrode, and a leakless Ag/AgCl reference electrode. A reducing potential is applied to the working electrode in the presence of 4-nitrophenyldiazonium hydrochloride, formed in situ by the presence of hydrochloric acid and sodium nitrite. The surface modification occurs rapidly and simultaneously reduces the aryl nitro group (NO_2 in red, Fig. 2) to the corresponding

Fig. 1 **A** A close-up of a turtle shell highlighting the hard-soft suture-shaped interface leading outstanding physical properties; **B** The approach taken to tailor reclaimed carbon fibre surface towards thermoset and thermoplastic polymers. The former employs an amine to crosslink with the epoxy resin (in red), generating a 'hard' interface. The latter uses a short alkyl (butyl) chain to entangle and complement the hydrocarbon backbone of polypropylene (in blue) (color figure online)



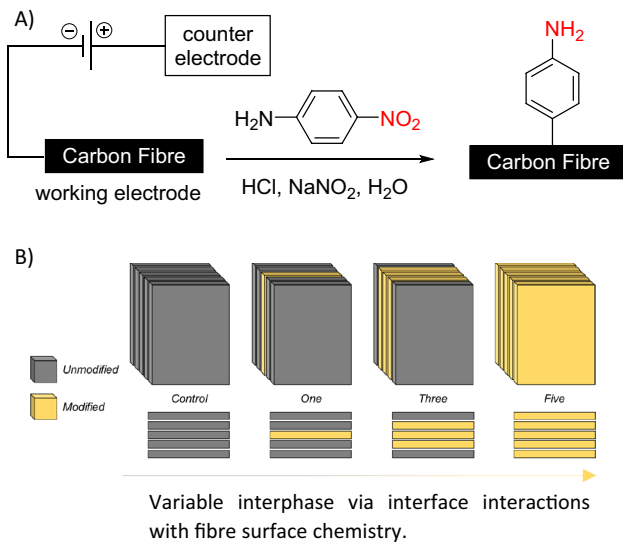


Fig. 2 **A** Electrochemical modification of reclaimed carbon fibre non-woven fabrics; **B** Lay up for thermoset composite samples

amine (NH_2 , in red, Fig. 2). This furnishes the carbon fibre fabric with exposed reactive nitrogen species on its surface. The fabrics were then washed with copious amounts of acetone, ethanol, and water to remove all unreacted material and salts.

The samples were laid up in the configurations outlined below (Fig. 2, B) whereby the modified plies (yellow) were increased from the centre ply at intervals of 0, 1, 3, and 5. The samples were impregnated with resin via vacuum infusion and cured in a compression mould to give plates from which the test coupons were obtained.

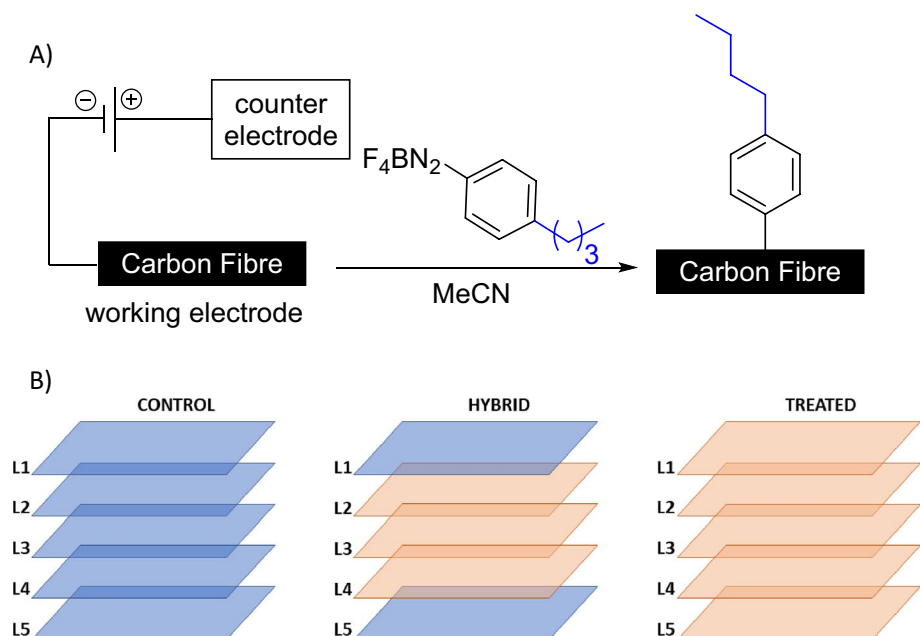
2.1.2 Thermoplastic Sample Preparation

The recycled non-woven carbon fibre substrate used for this study was IM56L CF/PP [38], sourced from Gen2Carbon, United Kingdom. The carbon fibre has a mean chopped fibre length range of 5 mm, an aerial weight of 220 g/m^2 , and carbon fibre content of 30 wt.% by weight, with the remainder being entangled polypropylene filaments. The electrochemical cell comprised of a carbon fibre/PP mat ($125 \times 125 \text{ mm}$, IM56L CF/PP non-woven) and the counter electrode was a non-woven carbon fibre fabric ($120 \text{ mm} \times 280 \text{ mm}$, G-TEX M 100 GSM, Gen 2 Carbon, United Kingdom). A leakless Ag/AgCl electrode (ET069-1, eDAQ Australia) was used as the reference electrode and affixed between the counter and working electrode.

The electrolyte comprised of a DMF: H_2SO_4 mixture ($1 \text{ M H}_2\text{SO}_4$) with *n*-butyl benzene diazonium tetrafluoroborate (745.6 mg , 3 mM) added and stirred until dissolved. A series of 10 voltametric sweeps between -1.0 V and 0 V (vs. Ag/AgCl) was applied at a scan rate of 10 mV/s . After the graft was complete, the working electrode was removed and washed in methylene chloride, ethanol, and acetone, followed by drying under reduced pressure overnight to remove any residual solvent (Fig. 3A). The non-conductive nature of the entangled polypropylene filaments ensures that chemical modification only occurred on the carbon filaments.

To fabricate the PP laminates, 5 layers of IM56L CF/PP were cut to into rectangular sections of $260 \text{ mm} \times 160 \text{ mm}$ and stacked. The hybrid interfaces were created by alternately layering functionalised and non-functionalised layers on top of each other (Fig. 3B) A control composite where all 5 layers were non-functionalised was prepared and used

Fig. 3 **A** Modification of CF/PP fabrics with *n*-butylphenyl groups; **B** Stacking sequence of 'control', 'hybrid', and 'treated' composites. (L denotes layer number, Blue denotes untreated CF/PP, Orange denoted functionalised CF/PP) (color figure online)



as received, while the ‘treated’ composite refers to the functionalisation of all 5 layers, while the ‘hybrid’ composite contained three inner functionalised layers. A visual representation of stacking sequence is presented in Fig. 3 illustrates the entire set of hybridised composites fabricated detailing the sequence of functionalised and non-functionalised layers.

Once stacked, the dry fabric laminates were placed into a hot press at a temperature of 260 °C and pressure of 472 kPa for 10 min. The platen heads on both sides were lined with a PTFE release film prior to pressing thereby ensuring the laminates could be removed. It is worth noting that during pressing, the polypropylene filaments were able to melt and infuse the laminate, producing a well consolidated void free composite. After pressing, the laminates were removed from the platen press and placed on a metal plate using a flat head scraper and allowed to cool to room temperature. Once fully cooled, the laminate was waterjet cut to produce testing coupons as per the dimensions provided in the accompanying ESI which are in accordance with appropriate ASTM standards (see Sect. 2.3).

2.2 Mechanical Testing

All mechanical testing within this study was conducted using a 50 kN Instron universal testing machine operative via BlueHill3 software.

Compressive testing was conducted in accordance with ASTM D6641 [39] where specimen dimensions were 13 mm in width, 140 mm in length and 3 mm in thickness. A combined loading compression (CLC) fixture was used to secure samples in place before a 1.3 mm/min displacement controlled compressive loaded was applied. Compressive strength and modulus of samples were determined as per equations in accompanying ESI.

Flexural testing was conducted in accordance with ASTM D2344 [40]. Specimen dimensions were 13 mm in width, 65 mm in length and 3 mm in thickness. A three-point bend fixture was used with roller and anvil diameters of 10 mm and a displacement-controlled loading of 2 mm/min. Flexural yield strength was determined via 0.2% strain offset, while ultimate flexural strength (σ_{UFS}) and flexural modulus were determined as per equations in accompanying ESI.

Double V-notch shear testing was completed in accordance with ASTM D5379 [41]. Specimens of 21.5 mm width, 75 mm length, 3 mm thickness and 5 mm notch depth either side of the samples were manufactured. An Iosipescu shear test fixture (Wyoming Fixtures, USA) was used to mount samples in place and a 2 mm/min compressive displacement force was then applied. Shear chord modulus and ultimate shear strength were recorded, respectively, as determined via equations in accompanying ESI.

Fracture toughness was conducted in accordance with ASTM D5045-14. Specimens 50 mm in length, 12 mm in width, 3 mm in thickness with a 4 mm in notch depth were produced. A three-point bend fixture with 10 mm roller diameters was used to stress the fracture coupons at a rate of 10 mm/min until failure was initiated at the notch front. Fracture toughness, modulus, and stress at failure were recorded as per equations in accompanying ESI.

The load, displacement, stress and strain data points for all testing was recorded at 10 microsecond intervals. Determination of statistically significant differences between data set was performed using two tailed, homoscedastic t-testing, with a P value less than 0.05 being considered a statistical change.

3 Results and Discussion

3.1 Thermoset Polymer Composites

The impact of increasing the number of functionalised plies from 1, 3 and 5, compared to the control sample containing no functionalised carbon fibre for the epoxy thermoset matrix was undertaken (Fig. 4). The control sample (i.e. no modified plies) exhibited a flexural strength of 314.1 ± 50.7 MPa and a flexural modulus of 10.9 ± 1.9 GPa. The five amine-modified composites gave an improved flexural strength of 387.5 ± 28.2 MPa, and an improved flexural modulus of 13.99 ± 0.82 GPa. Similarly, the sample featuring three amine-modified plies in its centre improved flexural strength to 399.0 ± 8.89 MPa and the flexural modulus to 14.82 ± 0.53 GPa. However, as per the flexural strength, the largest improvements for both flexural strength and flexural modulus were observed for the sample featuring only one modified ply through the centre of the composite, being 420.7 ± 13.1 MPa and 16.3 ± 1.0 GPa, respectively.

The trends for flexural strength were consistent with flexural modulus, where the sample with a single modified ply gave an average increase of 5.39 GPa (+49.43%) when compared to the control sample. The sample with three modified plies gave an average increase of 3.92 GPa (+35.94%) in flexural modulus, and the five modified ply sample saw an average improvement of 3.10 GPa (+28.42%) compared to the control.

Improvements to the average mechanical performance were observed for all samples featuring modified plies, with the single modified ply sample being significantly higher than the others. This speaks to a reinforcing effect resulting from the strategic placement of two different nonwoven surface chemistries within a composite. The abundance of amine-functionalised carbon fibres would encourage a higher degree of cross-linking from the resin to the fibre creating a strong interface. This effect could facilitate the

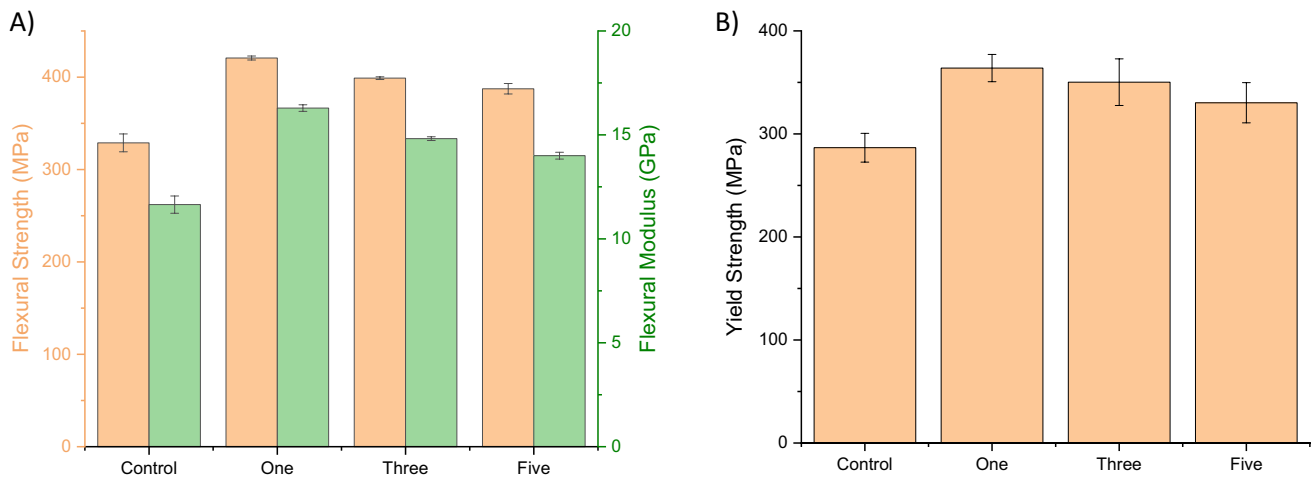


Fig. 4 **A** Flexural strength and modulus of samples possessing variable interface chemistries; **B** Increases in yield strength for samples with increasing amounts of aminated fibre

transfer of bending stresses between the fibre and its supporting matrix. The progressive decrease in flexural strength and modulus as plies increase is likely due to the increasingly brittle nature of the interface, which may fracture easily. This is consistent with observations made by our group when applying this ply modification strategy to virgin carbon fibres [42].

Similar improvements were seen in the yield strength of the samples. The largest improvement was observed for the sample with one modified ply, giving a yield strength of 363.95 ± 13.25 MPa, an increase of 27.3% compared to the control (286.6 ± 14.47 MPa). A smaller improvement of 22.5% (350.22 ± 22.62 MPa) was achieved for the three-ply sample, and only 330.25 ± 19.54 MPa for the five modified plies, an increase of 15.5%. These improvements indicate that incorporating amine-modified nonwoven fabrics into the laminate will delay the point of irreversible plastic deformation, with the largest increase coming from the single amine ply in the central laminate.

The trends observed in work using reclaimed carbon fibres support those reported elsewhere for virgin carbon fibre [35, 36] and to some degree, reflects the ease of enhancing compatibility between an epoxy matrix and carbon fibre due to the available functional groups during and after cure. For this reason, however, this hybrid functionalised interface approach was explored using a non-functional thermoplastic such as polypropylene to understand its wider utility.

3.2 Translating Variable Interface Chemistry to Polypropylene Matrix Composites

The surface modification approach of virgin carbon fibres to complement PP as described above, has been reported earlier where an increase in composite toughness was reported

[37]. Furthermore, the interfacial molecular interactions are significantly softer in this system (Van der Waals, etc.), compared to the epoxy thermoset network (hydrogen bonding, covalent, etc.). Therefore, a minimum of three modified samples were examined to encourage the easy identification of changes in physical properties. In these systems, synergistic enhancements between the hybrid laminate, compared to the treated and control composites was investigated for a range of different deformation approaches including compression, flexural, shear, and fracture properties were examined.

3.2.1 Compressive Properties

The evaluation of these composite materials under compressive loads was examined first (Fig. 5). Typically, the fibrous reinforcement provides minimal benefit in this stress state. Interestingly, a 63% increase in compressive strength (2.68 MPa; 4.27 ± 0.49 MPa to 6.95 ± 0.68 MPa) compared to the control sample for the fully modified composite, a 23% increase of 0.98 MPa (to 5.25 ± 0.68 MPa) was observed, relative to unmodified control.

When evaluating compressive modulus (i.e. the resistance of the sample to compress), a small reduction of 0.35 MPa (−9.2%) lower than the control was observed. Hybrid samples exhibited compressive modulus 1.75 MPa (+45.3%) higher than the control sample and 2.10 MPa (+60.0%) larger than treated samples, respectively. The improvement in compressive strength and modulus are likely due to enhanced interfacial adhesion between the fibre and the resin. Other works have shown that as IFSS increases the compression strength of the composite also increases. This observation was found by Nairn [43], Drzal [44], and Stojcevski [45] in three separate reports, albeit focusing on polycarbonate, epoxy, and open hole compression, respectively.

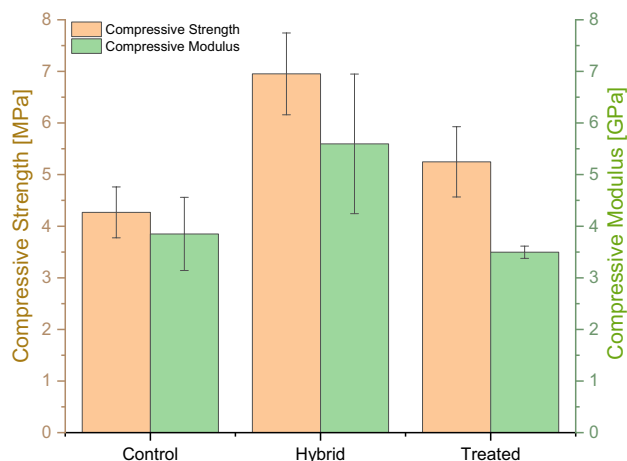


Fig. 5 Compressive strength (MPa) and compressive modulus (GPa) results of control, hybrid, and fully treated laminate arrangements

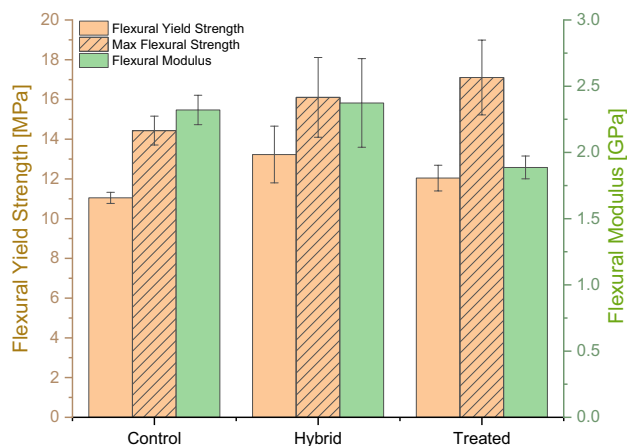


Fig. 6 Flexural yield strength (MPa), maximum flexural strength (MPa) and flexural modulus (GPa) of control, hybrid, and fully treated laminate arrangements

Moreover, Wang et al. examined carbon fibre-polypropylene composites, incorporating a maleic anhydride co-monomer, and observed improvements in IFSS based on molecular entanglement at the fibre–matrix interface [46].

3.3 Flexural Properties

The flexural yield strength, maximum flexural strength, and flexural modulus of control, hybrid and treated laminate variants were examined next for these specimens (Fig. 6). The yield strength of control, hybrid, and treated samples were 11.05 ± 0.28 MPa, 13.23 ± 1.43 MPa, and 12.0 ± 0.65 MPa, respectively. When compared to the yield strength of the control samples, hybrid laminates showed an increased yield strength by 2.18 MPa (+ 19.7%), whereas the treated laminated increased yield strength by

0.99 MPa (+ 9.8%) (Fig. 6). When comparing the hybrid and treated samples, the hybrid was found to have a yield strength 1.19 MPa (+ 9.8%) greater than that of the treated. These changes in yield strength indicate that the stress required to initiate plastic deformation and subsequent strain hardening is altered by the fibre functionalisation process, and thus the corresponding fibre–matrix inter-phase/interface, of which the hybrid arrangement allowed for the greatest delay in plasticity.

When correlating that finding to ultimate flexural strength, treated samples provided the greatest strength of 17.11 ± 1.88 MPa, followed by the hybrid configuration at 16.10 ± 2.01 MPa and finally the control at 14.43 ± 0.72 MPa. These values correlate to a 1.76 MPa (+ 11.6%) increase in flexural strength for hybrid laminates, as compared to control samples (Fig. 6). Relative to the control samples, only the treated configuration showed a statistically relevant improvement, though the hybrid configuration was effectively indistinguishable from the treated.

The exchange between highest flexural yield strength and ultimate flexural strength performance between the hybrid and treated samples is of interest. While the hybrid laminate seems to delay plastic deformation onset for the longest elongation of all specimens, it is unable to reach the ultimate flexural strength of treated samples. As the 3-point bending introduces compressive, shear and tensile stress states concurrently, the inclusion of treated fibres in the central layers provides reinforcement where there is the greatest stress within the structure. This would account for the increased ultimate flexural strength, as the accompanying results within this study have shown the hybrid arrangement to perform highest in shear and compression at the expense of maximum flexural strength. When analysed under optical microscopy, all laminate samples (regardless of variant) were found to fail under tension and, in some cases, a mixture of shear plane failure and tension concurrently. This suggests that the tensile plane of the laminates, i.e. the bottom most portion of the composite being stressed, is the weakest point. This supports the premise that treated samples have improved ultimate flexural strength through reinforcement of the outermost plane experiencing tension.

The treated samples showed a flexural modulus 0.47 MPa (– 18.7%) below that of control samples and 0.49 MPa (– 25.8%) below that of hybrid samples (Fig. 6). This reduction in flexural modulus for treated samples coupled with the highest flexural strength highlights strain-hardening mechanisms to be influencing flexural performance [37, 47]. It is possible that through the surface treatment of carbon fibre, changes to the polypropylene entanglement, cohesive energy and laminar arrangements, and stiffness of fibre-to-matrix interphases may be occurring. This same phenomenon using identical surface chemistry was observed in a previous study

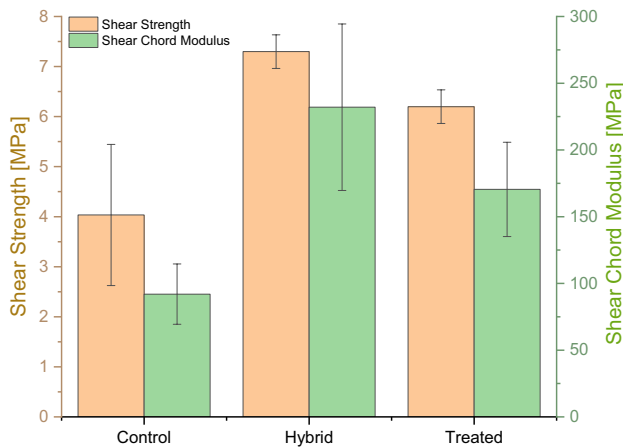


Fig. 7 Shear strength (MPa), and shear chord modulus (MPa) of control, hybrid, and fully treated samples. (* denotes statistical significance as compared to control condition)

[37]. Further comprehensive analysis into this occurrence is currently underway and the subject of future work.

3.4 Shear Properties

The shear strength and shear chord modulus of control, hybrid, and treated laminates was examined next (Fig. 7). Statistically significant differences in shear strength were observed across all three laminate variants. Control fibres possessing the lowest shear strength value at 4.03 ± 1.41 MPa, followed by treated samples with a shear strength of 6.20 ± 0.34 MPa, and hybrid samples provided the highest value of 7.30 ± 0.34 MPa. These increases in shear strength correlate to 3.26 MPa (+80.9%) and 2.16 MPa (53.6%) for hybrid and treated variants, respectively, relative to control samples. Accordingly, the associated increase in shear strength of hybrid samples as compared to treated samples was 1.10 MPa (+17.7%).

With respect to shear chord modulus, all laminate variants presented statistical differences in mechanical performance. Control, hybrid, and treated arrangements had shear chord moduli of 91.98 ± 22.58 MPa, 232.03 ± 62.40 MPa, and 170.47 ± 35.31 MPa, respectively. These values correlate to a 78.48 MPa (+85.3%) increase in modulus for treated laminates, and 140.04 MPa (+152.2%) increase in hybrid samples, respectively, as compared to control laminates. Similarly, hybrid laminates had a shear chord modulus 61.56 MPa (+36.1%) larger than that of treated specimens.

The double V-notch shear test used within this study is of note as it provides a state of pure shear stress across the loaded specimen where the sum of stresses in both the x and y axis are zero. As such, these results indicate that fibre-matrix adhesion within the laminate has improved through the surface modification of the carbon fibres and is in an

optimal state for the hybrid layup. This is in line with previous works into woven carbon fibre laminates [35, 36].

3.5 Fracture Properties

The fracture toughness and stress at failure for the control, hybrid and treated samples was determined next (Fig. 8). Fracture toughness was observed to increase by 63.2% from $0.12 \text{ MPa m}^{1/2}$ for control samples to $0.20 \text{ MPa m}^{1/2}$ for samples in the hybrid configuration. This trend was not observed for fully treated coupons which showed no statistically significant increase in fracture toughness as compared to control samples with a fracture toughness of $0.13 \text{ MPa m}^{1/2}$.

Interestingly, while the average values of stress experienced at failure followed the same trend in performance as that of the fracture toughness, there was no statistically significant differences. The stresses experienced at failure for control, hybrid and treated samples were 11.67 MPa, 13.89 MPa and 12.21 MPa, respectively (Fig. 8). This indicates that while the ability to dissipate energy within the samples varies dependant on laminate arrangement and functionalisation, the ultimate stress to cause failure at a pre-crack front does not change significantly.

3.6 Overview of Physical Properties

Overall, these results show that most mechanical properties are at their optimal when composites were arranged as ‘hybrid’ laminates (Fig. 9). When compared against control samples, significant improvements were observed for the hybrid configuration for shear chord modulus, fracture toughness and maximum compressive strength. Instances in which variance between control and hybrid samples were negligible were only fracture modulus and flexural modulus.

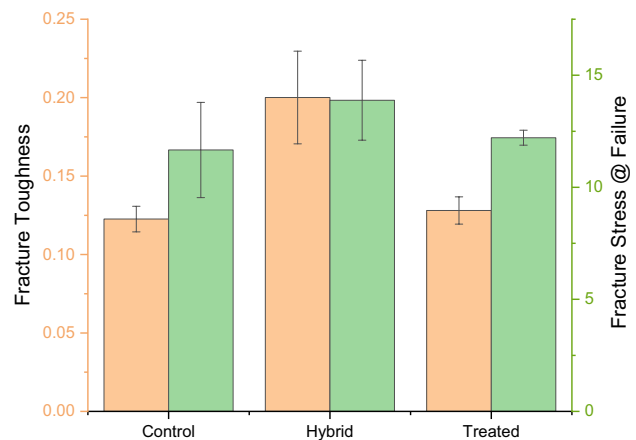
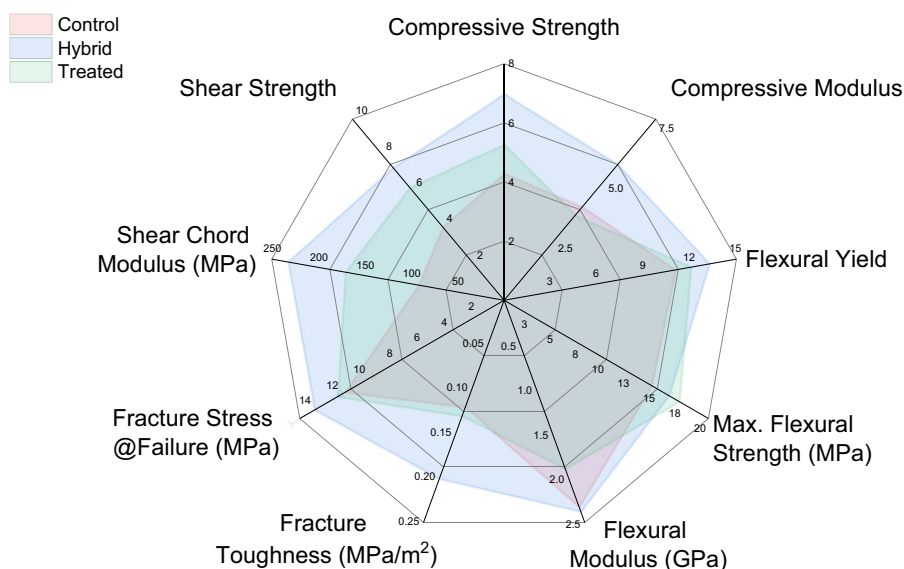


Fig. 8 Fracture toughness ($\text{MPa m}^{1/2}$), fracture modulus (GPa) and stress at failure (MPa) of control, hybrid, and fully treated samples

Fig. 9 Radar plot comparing the catalogue of mechanical properties investigated within this study with respect to ‘control’, ‘hybrid’, and ‘treated’ composite arrangement



The treated composite variant was found to similarly provide improvements to mechanical properties above the control samples particularly when comparing shear, flexural, and compressive strength. Fracture modulus and flexural strength were of note as the highest performing properties amongst the three arrangements for the treated condition. Overall, the use of surface functionalisation and its subsequent implementation into CF/PP laminates has shown clear improvements to the global performance of the composite.

4 Conclusion

We show the ability to tailor the surface chemistry of reclaimed carbon fibres towards both thermoset and thermoplastic matrix composites. The assembly of laminate composites, for both polymer systems, using variable interface mechanics resulted in significant improvements when a combination of surface chemistries was employed. In the thermoset system, improvements in flexural strength and modulus were observed when only one ply of modified fibre was incorporated through the centre of the laminate. Similarly, for CF-PP composites the incorporation of three surface modified layers through the centre of the laminate resulted in the greatest improvements in properties. Using this arrangement increases in compressive strength of 62.9%, compressive modulus of 45.3%, flexural yield strength of 19.7%, fracture toughness of 63.2%, shear chord modulus of 152.2%, and shear strength of 80.9% were recorded as compared to control samples. Specimens in which all layers of the composite were functionalised were found to perform highest only in ultimate flexural strength and fracture modulus with increases of 18.5% and 49.5%, respectively, as compared to control samples.

Supplementary Information The online version contains supplementary material available at <https://doi.org/10.1007/s12221-023-00265-x>.

Acknowledgements The authors would like to thank the Australian Research Council (DP220100130) and the ARC Research Hub for Functional and Sustainable Fibres (IH210100023) for support. This work was partially funded by the office of naval research global (N62909-18-1-2024), and we thank Gen2Carbon for the raw materials.

Funding Open Access funding enabled and organized by CAUL and its Member Institutions.

Data availability Data is available upon request.

Declarations

Conflict of Interest The authors have no competing interests to declare.

Open Access This article is licensed under a Creative Commons Attribution 4.0 International License, which permits use, sharing, adaptation, distribution and reproduction in any medium or format, as long as you give appropriate credit to the original author(s) and the source, provide a link to the Creative Commons licence, and indicate if changes were made. The images or other third party material in this article are included in the article's Creative Commons licence, unless indicated otherwise in a credit line to the material. If material is not included in the article's Creative Commons licence and your intended use is not permitted by statutory regulation or exceeds the permitted use, you will need to obtain permission directly from the copyright holder. To view a copy of this licence, visit <http://creativecommons.org/licenses/by/4.0/>.

References

1. A.P. Mouritz, *Introduction to aerospace materials* (Elsevier, Amsterdam, 2012)
2. R.J. Tapper, M.L. Longana, A. Norton, K.D. Potter, I. Hamerton, An evaluation of life cycle assessment and its application to the closed-loop recycling of carbon fibre reinforced polymers. *Compos. B Eng.* **184**, 107665 (2020)

3. H. Ahmad, A. Markina, M. Porotnikov, F. Ahmad, A review of carbon fiber materials in automotive industry, IOP Conference Series: Materials Science and Engineering, IOP Publishing, 2020, p. 032011.
4. J. Zhang, V.S. Chevali, H. Wang, C.-H. Wang, Current status of carbon fibre and carbon fibre composites recycling. *Compos. Part B Eng.* **193**, 108053 (2020). <https://doi.org/10.1016/j.compositesb.2020.108053>
5. M. Sharma, S. Gao, E. Mäder, H. Sharma, L.Y. Wei, J. Bijwe, Carbon fiber surfaces and composite interphases. *Compos. Sci. Technol.* **102**, 35–50 (2014). <https://doi.org/10.1016/j.compscitech.2014.07.005>
6. S. Feih, A.P. Mouritz, Tensile properties of carbon fibres and carbon fibre–polymer composites in fire. *Compos. A Appl. Sci. Manuf.* **43**(5), 765–772 (2012). <https://doi.org/10.1016/j.compositesa.2011.06.016>
7. D.J. Eyckens, F. Stojceviski, A. Hendlmeier, J.D. Randall, D.J. Hayne, M.K. Stanfield, B. Newman, F. Vukovic, T.R. Walsh, L.C. Henderson, Carbon fiber surface chemistry and its role in fibre-to-matrix adhesion. *J. Mater. Chem. A* **9**(47), 26528–26572 (2021). <https://doi.org/10.1039/D1TA07151C>
8. S. Blassiau, A. Thionnet, A.R. Bunsell, Micromechanisms of load transfer in a unidirectional carbon fibre–reinforced epoxy composite due to fibre failures. Part 1: Micromechanisms and 3D analysis of load transfer: the elastic case. *Compos. Struct.* **74**(3), 303–318 (2006). <https://doi.org/10.1016/j.compstruct.2005.04.013>
9. S. Kotanen, T. Laaksonen, E. Sarlin, Feasibility of polyamines and cyclic carbonate terminated prepolymers in polyurethane/polyhydroxyurethane synthesis. *Mater. Today Commun.* **23**, 100863 (2020). <https://doi.org/10.1016/j.mtcomm.2019.100863>
10. J.D. Randall, D.J. Eyckens, E. Sarlin, S. Palola, G.G. Andersson, Y. Yin, F. Stojceviski, L.C. Henderson, Mixed surface chemistry on carbon fibers to promote adhesion in epoxy and PMMA polymers. *Ind. Eng. Chem. Res.* **61**(4), 1615–1623 (2022). <https://doi.org/10.1021/acs.iecr.1c04409>
11. S. Palola, P. Laurikainen, S. García-Arrieta, E. Goikuria Astorkia, E. Sarlin, Towards sustainable composite manufacturing with recycled carbon fiber reinforced thermoplastic composites. *Polymers*, 2022.
12. C. Pramanik, D. Nepal, M. Nathanson, J.R. Gissing, A. Garley, R.J. Berry, A. Davijani, S. Kumar, H. Heinz, Molecular engineering of interphases in polymer/carbon nanotube composites to reach the limits of mechanical performance. *Compos. Sci. Technol.* **166**, 86–94 (2018). <https://doi.org/10.1016/j.compscitech.2018.04.013>
13. A. Paipetis, C. Galiotis, Effect of fibre sizing on the stress transfer efficiency in carbon/epoxy model composites. *Compos. A Appl. Sci. Manuf.* **27**(9), 755–767 (1996). [https://doi.org/10.1016/1359-835X\(96\)00054-1](https://doi.org/10.1016/1359-835X(96)00054-1)
14. S. Bekah, R. Rabiei, F. Barthelat, The micromechanics of biological and biomimetic staggered composites. *J. Bionic Eng.* **9**(4), 446–456 (2012). [https://doi.org/10.1016/s1672-6529\(11\)60145-5](https://doi.org/10.1016/s1672-6529(11)60145-5)
15. H.D. Espinosa, J.E. Rim, F. Barthelat, M.J. Buehler, Merger of structure and material in nacre and bone—perspectives on de novo biomimetic materials. *Prog. Mater. Sci.* **54**(8), 1059–1100 (2009). <https://doi.org/10.1016/j.pmatsci.2009.05.001>
16. Z. Shao, F. Vollrath, Surprising strength of silkworm silk. *Nature* **418**(6899), 741–741 (2002). <https://doi.org/10.1038/418741a>
17. S. Keten, Z. Xu, B. Ihle, M.J. Buehler, Nanoconfinement controls stiffness, strength and mechanical toughness of beta-sheet crystals in silk. *Nat Mater* **9**(4), 359–367 (2010). <https://doi.org/10.1038/nmat2704>
18. K. Piekarski, Analysis of bone as a composite material. *Int. J. Eng. Sci.* **11**(6), 557–565 (1973). [https://doi.org/10.1016/0020-7225\(73\)90018-9](https://doi.org/10.1016/0020-7225(73)90018-9)
19. D. Nepal, S. Kang, K.M. Adstedt, K. Kanhaiya, M.R. Bockstaller, L.C. Brinson, M.J. Buehler, P.V. Coveney, K. Dayal, J.A. El-Awady, L.C. Henderson, D.L. Kaplan, S. Keten, N.A. Kotov, G.C. Schatz, S. Vignolini, F. Vollrath, Y. Wang, B.I. Yakobson, V.V. Tsukruk, H. Heinz, Hierarchically structured bioinspired nanocomposites. *Nat. Mater.* (2022). <https://doi.org/10.1038/s41563-022-01384-1>
20. Z.R. Yue, W. Jiang, L. Wang, S.D. Gardner, C.U. Pittman, Surface characterization of electrochemically oxidized carbon fibers. *Carbon* **37**(11), 1785–1796 (1999). [https://doi.org/10.1016/S0008-6223\(99\)00047-0](https://doi.org/10.1016/S0008-6223(99)00047-0)
21. J. Jiang, X. Yao, C. Xu, Y. Su, L. Zhou, C. Deng, Influence of electrochemical oxidation of carbon fiber on the mechanical properties of carbon fiber/graphene oxide/epoxy composites. *Compos. A Appl. Sci. Manuf.* **95**, 248–256 (2017). <https://doi.org/10.1016/j.compositesa.2017.02.004>
22. A. Fukunaga, S. Ueda, Anodic surface oxidation for pitch-based carbon fibers and the interfacial bond strengths in epoxy matrices. *Compos. Sci. Technol.* **60**(2), 249–254 (2000). [https://doi.org/10.1016/S0266-3538\(99\)00118-9](https://doi.org/10.1016/S0266-3538(99)00118-9)
23. C.U. Pittman, W. Jiang, Z.R. Yue, S. Gardner, L. Wang, H. Toghiani, C.A. Leon y Leon, Surface properties of electrochemically oxidized carbon fibers. *Carbon* **37**(11), 1797–1807 (1999). [https://doi.org/10.1016/S0008-6223\(99\)00048-2](https://doi.org/10.1016/S0008-6223(99)00048-2)
24. J. Gulyás, E. Földes, A. Lázár, B. Pukánszky, Electrochemical oxidation of carbon fibres: surface chemistry and adhesion. *Compos. A Appl. Sci. Manuf.* **32**(3), 353–360 (2001). [https://doi.org/10.1016/S1359-835X\(00\)00123-8](https://doi.org/10.1016/S1359-835X(00)00123-8)
25. M. Kanerva, L.S. Johansson, J.M. Campbell, H. Revitzer, E. Sarlin, T. Brander, O. Saarela, Hydrofluoric–nitric–sulphuric-acid surface treatment of tungsten for carbon fibre-reinforced composite hybrids in space applications. *Appl. Surf. Sci.* **328**, 418–427 (2015). <https://doi.org/10.1016/j.apsusc.2014.12.036>
26. D. He, V.K. Soo, F. Stojceviski, W. Lipiński, L.C. Henderson, P. Compston, M. Doolan, The effect of sizing and surface oxidation on the surface properties and tensile behaviour of recycled carbon fibre: an end-of-life perspective. *Compos. Part A Appl. Sci. Manuf.* **138**, 106072 (2020). <https://doi.org/10.1016/j.compositesa.2020.106072>
27. S.S. Pawar, S.A. Hutchinson, D.J. Eyckens, F. Stojceviski, D.J. Hayne, T.R. Gengenbach, J.M. Razal, L.C. Henderson, Carbon fiber sizing agents based on renewable terpenes. *Compos. Sci. Technol.* **220**, 109280 (2022). <https://doi.org/10.1016/j.compscitech.2022.109280>
28. N.G. Karli, C. Ozkan, A. Aytac, V. Deniz, Effects of sizing materials on the properties of carbon fiber-reinforced polyamide 6,6 composites. *Polym. Compos.* **34**(10), 1583–1590 (2013). <https://doi.org/10.1002/pc.22556>
29. F. Gnädinger, P. Middendorf, B. Fox, Interfacial shear strength studies of experimental carbon fibres, novel thermosetting polyurethane and epoxy matrices and bespoke sizing agents. *Compos. Sci. Technol.* **133**, 104–110 (2016). <https://doi.org/10.1016/j.compscitech.2016.07.029>
30. M.A. Downey, L.T. Drzal, Toughening of carbon fiber-reinforced epoxy polymer composites utilizing fiber surface treatment and sizing. *Compos. A Appl. Sci. Manuf.* **90**, 687–698 (2016). <https://doi.org/10.1016/j.compositesa.2016.09.005>
31. F. Stojceviski, T.B. Hilditch, T.R. Gengenbach, L.C. Henderson, Effect of carbon fiber oxidization parameters and sizing deposition levels on the fiber–matrix interfacial shear strength. *Compos. A Appl. Sci. Manuf.* **114**, 212–224 (2018). <https://doi.org/10.1016/j.compositesa.2018.08.022>
32. F. Stojceviski, T.B. Hilditch, L.C. Henderson, A comparison of interfacial testing methods and sensitivities to carbon fiber surface treatment conditions. *Compos. A Appl. Sci. Manuf.* **118**, 293–301 (2019). <https://doi.org/10.1016/j.compositesa.2019.01.005>

33. A. Hendlmeier, F. Stojcevski, R. Alexander, S. Gupta, L.C. Henderson, Examining conductivity, current density, and sizings applied to carbon fibers during manufacture and their effect on fiber-to-matrix adhesion in epoxy polymers. *Compos. Part B Eng.* **179**, 107494 (2019). <https://doi.org/10.1016/j.compositesb.2019.107494>
34. L. Servinis, K.M. Beggs, C. Scheffler, E. Wölfel, J.D. Randall, T.R. Gengenbach, B. Demir, T.R. Walsh, E.H. Doeven, P.S. Francis, L.C. Henderson, Electrochemical surface modification of carbon fibres by grafting of amine, carboxylic and lipophilic amide groups. *Carbon* **118**, 393–403 (2017). <https://doi.org/10.1016/j.carbon.2017.03.064>
35. F. Stojcevski, J.D. Randall, L.C. Henderson, Using variable interfacial adhesion characteristics within a composite to improve flexural strength and decrease fiber volume. *Compos. Sci. Technol.* **165**, 250–258 (2018). <https://doi.org/10.1016/j.compscitech.2018.06.025>
36. F. Stojcevski, D.J. Eyckens, J.D. Randall, L.I. Marinovic, G. Méric, L.C. Henderson, Improved out-of-plane strength and weight reduction using hybrid interface composites. *Compos. Sci. Technol.* **182**, 107730 (2019). <https://doi.org/10.1016/j.compscitech.2019.107730>
37. J.D. Randall, F. Stojcevski, N. Djordjevic, A. Hendlmeier, B. Dharmasiri, M.K. Stanfield, D.B. Knorr, N.T. Tran, R.J. Varley, L.C. Henderson, Carbon fiber polypropylene interphase modification as a route to improved toughness. *Compos. Part A* **159**, 107001 (2022). <https://doi.org/10.1016/j.compositesa.2022.107001>
38. AeroExpo, CARBISO Technical Data Sheet, in: E. Composites. (Ed.) 2006, p. 2.
39. A.S.f.T. Materials, ASTM D6641 - Standard Test Method for Compressive Properties of Polymer Matrix Composite Materials Using a Combined Loading Compression (CLC) Test Fixture, 2017.
40. A.S.f.T. Materials, ASTM D2344 - Standard Test Method for Short-Beam Strength of Polymer Matrix Composite Materials and Their Laminates, 2006.
41. A.S.f.T. Materials, ASTM D5379 - Standard Test Method for Shear Properties of Composite Materials by the V-Notched Beam Method, 2021.
42. L.T. Drzal, M. Madhukar, Fibre-matrix adhesion and its relationship to composite mechanical properties. *J. Mater. Sci.* **28**(3), 569–610 (1993). <https://doi.org/10.1007/BF01151234>
43. P.R. Stone, J.A. Nairn, Interfacial toughness and its effect on compression strength in polycarbonate/carbon fiber composites. *Polym. Compos.* **15**(3), 197–205 (1994). <https://doi.org/10.1002/polb.750150305>
44. M.S. Madhukar, L.T. Drzal, Fiber-matrix adhesion and its effect on composite mechanical properties. III. Longitudinal (0°) compressive properties of graphite/epoxy composites. *J. Compos. Mater.* **26**(3), 310–333 (1992). <https://doi.org/10.1177/002199839202600301>
45. F. Stojcevski, D.J. Hayne, T. Hilditch, L.C. Henderson, Investigating interfacial adhesion and open-hole compressive (OHC) strength correlations for CFRPs via variations in sizing and oxidative surface treatment, *Composites, Part A* (2021) Under Review.
46. Y. Liu, X. Zhang, C. Song, Y. Zhang, Y. Fang, B. Yang, X. Wang, An effective surface modification of carbon fiber for improving the interfacial adhesion of polypropylene composites. *Mater. Des.* **88**, 810–819 (2015). <https://doi.org/10.1016/j.matdes.2015.09.100>
47. R.N. Haward, Strain hardening of high density polyethylene. *J. Polym. Sci. Part B: Polym. Phys.* **45**(9), 1090–1099 (2007). <https://doi.org/10.1002/polb.21123>